Hydrogel tapes for fault-tolerant strong wet adhesion

Yi Cao (caoyi@nju.edu.cn)
Nanjing University https://orcid.org/0000-0003-1493-7868
Bin Xue
Nanjing University
Jie Gu
Nanjing University
Wenting Yu
Nanjing University
Lan Li
Southeast University
Meng Qin
Nanjing University
Qing Jiang
Nanjing University
Wei Wang
Nanjing University https://orcid.org/0000-0001-5441-0302

Article

Keywords: gels, hydrogels tapes, biomedical applications

Posted Date: June 21st, 2021

DOI: https://doi.org/10.21203/rs.3.rs-602221/v1

Abstract

Fast and strong bio-adhesives are in high demand for many biomedical applications, including closing wounds in surgeries, fixing implantable devices, and haemostasis. However, most strong bio-adhesives rely on the instant formation of irreversible covalent crosslinks to provide strong surface binding. Repositioning misplaced adhesives during surgical operations may cause severe secondary damage to tissues. Here, we report hydrogel tapes that can form strong physical interactions with tissues in seconds and gradually form covalent bonds in hours. This timescale-dependent adhesion mechanism allows instant and robust wet adhesion to be combined with fault-tolerant convenient surgical operations. Specifically, inspired by the catechol chemistry discovered in mussel foot proteins, we develop an electrical oxidation approach to controllably oxidize catechol to catecholquinone, which reacts slowly with amino groups on the tissue surface. We demonstrate that the tapes show fast and reversible adhesion at the initial stage and ultrastrong adhesion after the formation of covalent linkages over hours for various tissues and electronic devices. Given that the hydrogel tapes are biocompatible, easy to use, and robust for bio-adhesion, we anticipate that they may find broad biomedical and clinical applications.

Main Text

Sutures have long been the first choice in surgery for haemostasis, wound closure, and integration of bioelectronic devices. [1,2] However, suturing may cause tissue damage or scars at the fixing points and is difficult to apply to tissues with complex structures (e.g., spinal cord and heart). Recently, bio-adhesives have emerged as potential alternatives to sutures, [3-6] as they are biocompatible, nontoxic and easy to use. [7,8] Depending on the formulation, bio-adhesives can be either glue-type[9-20] or tape-type[21-23] adhesives. Glue-type adhesives require a long curing process (hours to days) to establish strong cohesion and interfacial adhesion. This long curing time greatly limits their applications in scenarios that require rapid and strong adhesion, such as attaching bioelectric devices to a beating heart or instant haemostasis. [17,18] Tape-type adhesives can be instant and reversible, but the adhesion strength is typically low (<50 kPa) if they only form non-covalent bonds with the tissues. They are also prone to detach from surfaces due to swelling of the adhesives or bleeding from the tissue [24-28]. To circumvent these drawbacks, tape-type adhesives based on covalent surface bonding have been introduced. [29-31] These adhesives are mechanically robust and can function properly on dynamic surfaces or tissues bearing considerable tension. However, once covalent adhesion bonds are formed, the adhesives cannot be removed easily. [32-34] In particular, as most surgeries are operated on dynamic tissue surfaces, mispositioning tape-type adhesives is almost unavoidable. It remains challenging to develop bio-adhesives that can rapidly, robustly, and conformally integrate with various wet tissues or bioelectronic devices yet remain detachable if misplaced[35]. To meet these needs, a few strategies have been introduced. For example, Suo and coworkers implemented a photolysable bond to allow detachment of adhesives upon UV light illumination.[36] Zhao and coworkers introduced a disulfide bond into covalent linkages to render redox-controlled reversible detachment and attachment.[37] Despite the great success of

these methods, using additional triggers still makes detachment inconvenient. Moreover, the chemical reactions used for detachment are often slow and not fully reversible.

In nature, marine organisms, such as mussels, can strongly bind to various organic and inorganic surfaces by secreting various proteaceous adhesives containing dihydroxyl phenylalanine (dopa).[38-40] More importantly, they have evolved a special mechanism to control the adhesion strength at different timescales. In freshly secreted adhesive proteins, the catechol group of dopa forms non-covalent interactions with various substrates (i.e., charge-charge interactions, π-π interactions, cation-π interactions, coordination, hydrogen bonding and hydrophobic effects). [15,16,41] Then, dopa is gradually oxidized to dopaquinone and forms hydrogen bonds with unoxidized catechol groups as well as amino or carboxyl groups.[42] The aggregation of hydrophobic dopaquinone provides additional cohesion. Eventually, dopaquinone forms covalent linkages with primary amine and thiol groups slowly (in hours) to render strong adhesion. [43-46] This timescale-dependent adhesion is precisely regulated by the pH of the environment and the presence of enzymes.[47] Remarkably, through this complicated dopa chemistry, mussels can integrate simultaneous strong and instant adhesion with a fail-safe timing mechanism to prevent premature solidification in the secretory system or mistargeted adhesion. However, in many synthetic adhesives with catechol-containing polymers, the oxidation speed and products of dopa are not well regulated, leading to a mixture of various oxidation products.[48,49]

Inspired by the sophisticated oxidation process of dopa in mussels, we develop a novel electro-oxidation approach to controllably oxidize dopa to dopaquinone for the construction of hydrogel tapes that combine instant and robust adhesion with fault-tolerant operation. Compared to widely used chemical oxidization, electro-oxidation not only promotes the production of dopaquinone but also reduces the generation of dopa oligomers, allowing the dopa groups to be efficiently utilized for interfacial crosslinking. The resulting hydrogel tapes form instant strong adhesion with various organic and inorganic surfaces through non-covalent interactions. The tapes can be repositioned multiple times without showing an obvious decrease in binding strength. After gradually forming covalent linkages, the hydrogel tapes show an increased adhesion strength of ~1268 J m^{-2}, outperforming many reported bio-adhesives. [50-55] We further demonstrate the feasibility of using the hydrogel tapes as tissue sealants and adhesives for soft and implantable devices both in vitro and in vivo. Finally, we show that the hydrogel tapes are biocompatible, degradable and suitable for various biomedical applications.

Results And Discussion

Design and mechanism of the hydrogel tape

The adhesive hydrogel tapes were made of bovine serum albumin (BSA), electro-oxidized alginate-dopa (see Fig. S1 for synthesis details) and polyacrylic acid (PAA) (Fig. 1). The hydrogels were covalently crosslinked between the amino groups on the BSA surface and the carboxyl groups of alginates and/or PAA in the presence of N-hydroxy succinimide (NHS) and 1-(3-dimethylaminopropyl)-3-ethylcarbodiimide hydrochloride (EDC). The entanglement of the polymers as well as the hydrogen bonding among dopa,

amine, and carboxyl groups provided physical crosslinks (top panel of Fig. 1). Moreover, PAA can absorb surface water, facilitating the formation of instant, dynamic, and strong interfacial bonds with dopa (middle panel of Fig. 1). [30] The alginate-dopa was partially electrically oxidized using a galvanic cell prior to hydrogel preparation (Fig. S2), and electro-oxidation ensured that most of the products were dopaquinone, which was in sharp contrast to the chemical oxidation products (Fig. S3). Dopaquinone on hydrogel surfaces can form covalent bonds with amino groups on tissue surfaces to establish long-term strong adhesion (bottom panel of Fig. 1). The dopaquinone inside the hydrogels can form hydrogen bonds with unoxidized dopa and covalent bonds with the amino groups on BSA surfaces to further strengthen the hydrogel network (Fig. 1). The hydrogels containing electro-oxidized alginate-dopa are named Electro-Ox hydrogels hereafter. The chemical oxidation of dopa by potassium periodate (KIO_4) mainly led to the formation of catechol dimers that cannot form covalent bonds with amino or thiol groups (Fig. S3). For comparison, hydrogels containing unoxidized alginate-dopa or chemically oxidized alginate-dopa (named Non-Ox and Chem-Ox hydrogels, respectively) were also studied. All hydrogels were prepared in tape format and were sandwiched between two thermoplastic polyurethane (TPU) patches before use.

Structure and physical properties

We first characterized the structure and physical properties of the hydrogel tapes. Thanks to the excellent flexibility, the hydrogels can be fabricated into various forms such as bandage like strips ad double-side tape like rolls (Fig. 2a). The colour of the Chem-Ox and Electro-Ox hydrogels was darker than that of the Non-Ox hydrogels due to the oxidation of dopa (Fig. 2b). Scanning electron microscopy (SEM) images indicated that the pore sizes of the Electro-Ox and Chem-Ox hydrogels were smaller than those of the Non-Ox hydrogels, presumably due to their higher crosslinking density (Fig. S4). The swelling ratios and solid contents of the three hydrogels were comparable (Fig. S5). Due to the high crosslinking density of the Electro-Ox hydrogel tapes, their maximum swelling ratios were in the range of 2.5-3.2. This property greatly prevented the delamination of tape from wet tissues during long-term in vivo applications.

We then measured the mechanical properties of the hydrogel tapes. The Electro-Ox hydrogel tapes could be stretched to more than seven times the original length without causing any cracks (Fig. 2c), demonstrating their high stretchability. The fracture strain and fracture stress of the Electro-Ox hydrogel tapes were significantly higher than those of the Chem-Ox and Non-Ox hydrogel tapes (Fig. 2d and S6a). The toughness of the Electro-Ox hydrogel reached 22.6 MJ m^{-3} (Fig. S6b). The stress-strain curves of all hydrogel tapes exhibited obvious hysteresis, suggesting that the tapes contained abundant non-covalent interactions that can be ruptured upon stretching to dissipate energy (Fig. 2e and S6c). The Electro-Ox hydrogel tapes exhibited the highest dissipated energy (0.13 MJ m^{-3}) and the largest dissipation ratio (72.6%). We further optimized the mechanical properties of the Electro-Ox hydrogel tapes by varying the amount of alginate-dopa (Fig. 2f) or the total solid content (Fig. S7). The Young's modulus increased with increasing alginate-dopa or total mass concentrations (Fig. S6d and S7b). However, the maximum strain was negatively correlated with the total mass concentration.[56,57] Therefore, the highest fracture

energy was achieved at an alginate-dopa concentration of 10% (w/v) and a total solid content of 50% (w/v) (Fig. S6-S7). The high mechanical strength and toughness as well as the significant energy dissipation make the hydrogel tapes suitable for strong adhesion. [58]

Adhesion performance

Next, the adhesion performance of the Electro-Ox hydrogel tapes was evaluated at different timescales. We used wet porcine skin as the model tissue because its mechanical and biological properties are similar to those of human skin.[59] We first allowed two pieces of porcine skin to adhere using Electro-Ox hydrogel tape for less than 10 seconds and measured the adhesion strength under cyclic attachment/detachment at a short timescale (Fig. 3a). The adhesion strength was ~28 kPa for the first cycle, decreased slightly to 90% after 6 cycles, and decreased to ~66% after 20 cycles (Fig. 3b). We also studied whether the adhesion strength in the second cycle was affected by the time that the adherends remained formed in the previous cycle before being detached (Fig. 3c). The adhesion strength in the second cycle retained more than 70% of the initial value when the tape was adhered for 20 min and was still ~50% when the tape was adhered for 1 h. These results confirmed that the Electro-Ox hydrogel tapes have a strong instant binding strength and are detachable and reusable.

We then used three different types of mechanical tests (peel test for interfacial toughness, lap shear test for shear strength, and tensile test for tensile strength) to evaluate the long-term adhesion performance of the hydrogel tapes after being adhered for 24 h (Fig. 3d-f and Fig. S8) [29]. As summarized in Fig. 3f, the shear and tensile strength between the Electro-Ox hydrogel tape and the wet porcine skin were ~1.46 MPa and 1.25 MPa, respectively. The interfacial toughness of the Electro-Ox hydrogel tape and the porcine skin reached 1268 J m^{-2}. This high shear strength, tensile strength, and interfacial toughness indicated that the Electro-Ox hydrogel tape can establish strong and tough adhesion between wet porcine skin samples. In contrast, the shear strength, tensile strength, and interfacial toughness of the Chem-Ox (shear strength: 0.68 MPa, tensile strength: 0.62 MPa, interfacial toughness: 0.45 kJ m^{-2}) and non-Ox hydrogel tapes (shear strength: 0.24 MPa, tensile strength: 0.87 MPa, interfacial toughness: 0.23 kJ m^{-2}) were significantly smaller due to the presence of less dopaquinone than that in the Electro-Ox hydrogel tape. Moreover, the adhesion strength could be further optimized by varying the composition and electro-oxidation time (Fig. S9). We then characterized the mechanical stability of long-term tissue adhesion by the Electro-Ox hydrogel tape under a dynamic mechanical load. Two pieces of wet porcine skin joined by hydrogel tape were cyclically stretched to 20% strain and then relaxed (Fig. S10a). The shear strength slightly decreased with increasing cycle number and retained more than 85% of the original value even after 5000 cycles, further demonstrating the long-term stability of the hydrogel tapes in a dynamic mechanical environment (Fig. S10b-c).

We then evaluated the short-term and long-term shear strength between the Electro-Ox hydrogel tapes and various ex vivo tissues, including porcine vessels, stomach, liver, intestine, and heart. As shown in Fig. 3g

and h, the shear strength for short-term adhesion (less than 10 s) was higher than 30 kPa for all tissues (~78 kPa for vessels, ~31 kPa for the stomach, ~32 kPa for the liver, ~33 kPa for the intestine, and ~40 kPa for the heart), and the shear strength for long-term adhesion (24 hours) was higher than 100 kPa (~250 kPa for vessels, ~130 kPa for the stomach, ~155 kPa for the liver, ~101 kPa for the intestine, and ~144 kPa for the heart). The adhesion strength of Electro-Ox hydrogel tapes was not affected by the blood on tissue surfaces (Fig. S11). Moreover, serum proteins that had been adsorbed into the hydrogels can react with dopaquinone to provide additional crosslinks and reduce the swelling ratio of the hydrogel tape (Fig. S12). These features make Electro-Ox hydrogels ideal candidates for haemostatic dressings. The Electro-Ox hydrogel can also establish stable adhesion between wet tissues and other solid surfaces that are widely found in various electronic devices (Fig. 3i). The shear strength of the long-term adhesion reached 803, 243, 390, and 249 kPa for iron (Fe), silicon dioxide (SiO_2), polymethyl methacrylate (PMMA), and glass substrates, respectively.

Potential applications

We next evaluated the potential applications of the Electro-Ox hydrogel tape for tissue adhesion using ex vivo porcine tissue models. The Electro-Ox hydrogel tape can be applied to seal a water-leaking stomach (Fig. 4a and movie S1) and air-leaking lung (Fig. 4c and movie S2) in 30 s. Moreover, the sealed stomach and lung can perfectly hold water or air without any leakage after sealing, as monitored using the changes in water level and volume (Fig. 4b and d). Electro-Ox hydrogel tape can also be used to adhere devices onto tissue surfaces to monitor dynamic motion. As an example, we adhered a capacitive strain sensor on a porcine heart via Electro-Ox hydrogel tape (Fig. 4e). The heart was cyclically pressurized by intermittent airflow to mimic heartbeats. The strain sensor attached to the beating heart surface could monitor the motion of the heart through the synchronous deformation of the pericardium, the Electro-Ox hydrogel tape and the flexible sensor (Fig. 4f and movie S3).We further evaluated whether the hydrogel tapes were suitable for in vivo adhesion and haemostasis. After being pressed for 7 s, the Electro-Ox hydrogel tape stably adhered to a rabbit gastrocnemius surface (Fig. 5a). After implantation for 3 d in vivo, the hydrogel tape reached swelling equilibrium and remained adhered on the surface (Fig. 5b and movie S4). When the hydrogel tape was peeled off, the fracture appeared inside the hydrogel layer instead of at the surface. We further adhered a metal sheet (weight of ~ 0.52 g and diameter of ~9 mm) to the epicardial surface of a beating rabbit heart using Electro-Ox hydrogel tape to mimic device adhesion in vivo (Fig. 5c). The metal sheet stably adhered to the beating heart after gentle pressing for 7 s (Fig. 5d and movie S5). After beating for 3 h (~36,000 beats), the metal sheet still adhered at the same position. These results demonstrate the suitability of applying this hydrogel tape for many challenging in vivo applications. Furthermore, we evaluated the haemostasis of the bleeding carotid artery of a living pig using Electro-Ox hydrogel tape (Fig. 5e). After gently compressing the Electro-Ox hydrogel tape on a bleeding carotid artery, the bleeding was stopped without any leakage (Fig. 5f and movie S6). These results demonstrated that the hydrogel combines great mechanical strength, rapid surface bonding, and long-term mechanical stability and is suitable for applications in dynamic and stress-bearing tissues.

Biocompatibility and biodegradability

Finally, we investigated the biocompatibility and biodegradability of the Electro-Ox hydrogel tape in vitro and in vivo (Fig. 6). For the in vitro biocompatibility tests, mouse embryo osteoblast (MC 3T3) cells and mouse embryonic fibroblast (MEF) cells were cultured on Electro-Ox hydrogels for 24 h before the cell viabilities were determined using live/dead cell staining (Fig. 6a). Nearly no dead cells could be observed on the hydrogel tapes for both cells, and the cell viability was >95% compared to the control group (Fig. 6b and S13). Moreover, the Electro-Ox hydrogel showed protease-dependent degradability. The Electro-Ox hydrogel tape remained stable when placed in phosphate buffer solution (PBS) or simulated body fluid (SBF) buffer at 37 °C for 10 d (Fig. 6c). Upon the addition of collagenase, the hydrogel tape quickly lost 40% of its weight in 10 d.

We finally evaluated the in vivo biocompatibility and biodegradability of the tape based on dorsal subcutaneous implantation in a rabbit model (Fig. 6d and e). As indicated by the histological assessment results after implantation for 1, 2, 3, and 4 weeks, the hydrogel tapes did not cause any major damage to the surrounding dermal and muscular layers. Moreover, neither necrosis of the skeletal muscle and skin nor an eosinophilic response was observed (Fig. 6d and S14a). A mild chronic inflammatory response could be found, as indicated by the presence of macrophages, lymphocytes, and occasional giant cells. The inflammatory response was considerably weakened with increasing time. Even though the hydrogel tapes maintained ribbon-like structures after four weeks of implantation, they became obviously thinner (Fig. S14c) and started to split at the edges. We further performed immunofluorescence staining of tumour necrosis factor α (TNF-α) to evaluate the inflammatory response (Fig. 6e and S14b). The results indicated a low expression level of TNF-α and mild inflammation around the hydrogel tapes (Fig. S14d). All these results suggested the great biodegradability and weak inflammatory response of the Electro-Ox hydrogel tapes in vivo.

Conclusions

In this work, we report mechanically robust hydrogel tapes suitable for rapid and strong adhesion to various wet tissues and solid electronic devices. In contrast to other hydrogel tapes that use fast surface covalent bonding (e.g., EDC/NHS-catalysed amide bond formation), we introduced a slow covalent bonding reaction between dopaquinone and the amino groups of wet tissue surfaces. Due to the moderate reaction rate, the tapes can be repositioned multiple times without showing an obvious decrease in binding strength relative to the initial value. Moreover, the hydrogel tapes showed a great adhesion strength of ~ 1268 kJ m^{-2} after covalent linkages were formed in hours, outperforming many reported bio-adhesives. The great blood adsorbing ability of the hydrogel tapes allows them to function properly on blood covered surfaces. We further demonstrated the successful use of the hydrogel tapes as tissue sealants and adhesives for wearable and implantable devices, even on dynamic and bleeding tissue surfaces. The hydrogel tapes were biocompatible, degradable and suitable for various biomedical applications. The demonstration of the combination of instant and strong wet adhesion with fault-

tolerant practical surgical operation may inspire the design of next-generation hydrogel tapes that can function in challenging surgical conditions.

Methods

Preparation of hydrogel

In a typical preparation of the hydrogel, BSA, PAA and dopa-containing polymer (electro-oxidized, chemically oxidized or unoxidized alginate-dopa) were dissolved in ddH_2O to concentrations of 20, 60 and 20 mg mL^{-1}, respectively. Then, 25 mL of the mixture was dried in a petri dish (diameter of 60 mm) for 24 hours at 3% humidity and 25 °C to obtain dry tape samples. Then, PBS solution (5 mL) containing EDC (100 mM) and NHS (100 mM) was applied to the tape to crosslink the BSA, PAA and alginate. The hydrogel tape was transferred into ddH_2O to achieve swelling equilibrium for 24 hours, during which time the ddH_2O was refreshed more than 6 times to remove the unreacted reactants. Finally, the obtained hydrogels were stored in a mixture of alcohol (75%) and ddH_2O (25%) at room temperature before the experiments.

Tensile test

Tensile stress-strain measurements of the hydrogels were performed using a tensile-compressive tester (Instron-5944 with a 10 N sensor) in air at room temperature. Unless otherwise stated, the strain rate of stretching was maintained at ~10 mm min^{-1} (1.0 mm mm^{-1}). The strain, λ, was defined by the distance displacement between the two clamps when the gel was deformed divided by the distance when the gel was undeformed. The Young's modulus corresponded to the approximate linear fitting value at a strain of 20%. The toughness was calculated from the area below the tensile stress-strain curve until fracture.

Adhesion measurements

Fresh tissue samples were covered with PBS and stored in plastic bags at 4 °C before measurement. All the samples were prepared with the hydrogel sandwiched between the tissues and pressed for 30 seconds at a pressure of approximately 1.5 kPa. Then, adhesion measurements were performed after 24 h to allow equilibrium swelling of the hydrogels in a wet environment. All adhesion measurements were performed using a mechanical testing machine (2 kN load cell, Instron 5944, US).

For the shear strength measurements, the width and length of the adhesion areas were approximately 8 and 10 mm, respectively. All experiments were conducted in air at 25 °C with a constant stretching rate of 50 mm min^{-1} (Fig. 3d and e). The shear strength was determined as the maximum stress during the lap shear progress. For the interfacial toughness measurements, the samples were adhered with a width of 10 mm and tested by standard 180-degree peel tests (Fig. S8a and b). All experiments were conducted in air at 25 °C with a constant stretching rate of 50 mm min^{-1}. The interfacial toughness was determined as two times the plateau stress. For the tensile strength measurements, the width and length of the adhesion area were approximately 8 and 8 mm, respectively. All experiments were conducted in air at 25 °C

with a constant stretching rate of 50 mm min^{-1} (Fig. S8c and d). The tensile strength was determined as the maximum stress during the tensile stretching process.

For the cyclic stretch-relaxation test, two porcine skin tissues were adhered using the Electro-Ox hydrogel with an adhesion area of width 15 mm and length 30 mm. Then, the adhered samples were cyclically stretched to a strain of 20% with an initial hydrogel length of 100% and released to the original length. After different numbers of loading cycles, the shear strength of the samples was determined using the shear strength measurements and normalized to the initial shear strength. During the tests, PBS was sprayed onto the samples using a humidifier to avoid dehydration.

In vitro and in vivo biodegradation

In a typical biodegradation test in vitro, the hydrogel was cut into pieces with the same volume (0.5 mL), and the original dry weight of each hydrogel after washing with ddH_2O was defined as W_0. Then, a piece of Electro-Ox hydrogel (0.5 mL) was soaked in 50 mL of PBS (10 mM, pH=7.4), SBF or SBF containing 0.5 mM collagenase. The sample was incubated at 37 °C with a shaking rate of 220 r.p.m. At a certain time (t), the hydrogel was taken from the incubation medium and washed with ddH_2O three times. The sample was lyophilized, and the weight was defined as W_t. The weight loss at time t was determined as

$$\varepsilon = \frac{W_0 - W_t}{W_0} \times 100\%.$$

For in vivo biodegradation, hydrogel tapes with a width of 5 mm and length of 10 mm were prepared and stored in a mixture of alcohol (75%) and ddH_2O (25%) prior to implantation. Then, the mices (C57BL/6 mouse, n=20) were anaesthetized with the injection of isoflurane. The back hair of the rats was removed, and each sample was inserted between the skin and muscle through a 1.5 cm skin incision in the centre of the rat's back. Then, the incision was closed using interrupted sutures (3-0 Vicryl Plus, JNJ). After 1, 2, 3 or 4 weeks, 4 of the rats were sacrificed, and target subcutaneous regions were obtained and fixed in 10% formalin for 24 h before histological analyses and TNF-α immunofluorescent staining.

In vitro tissue adhesion and haemostasis

To evaluate the application of the Electro-Ox hydrogel in tissue adhesion and haemostasis, a series of in vitro experiments were performed. For the sealing of a damaged stomach, a hole with a diameter of 10 mm was made in a porcine stomach. A bottle of water was poured into the stomach to show water leakage. Then, Electro-Ox hydrogel tape (diameter: 30 mm) was applied to the hole and waited for 25s. Upon pouring water into the stomach again, the leakage stopped. The water level inside was also monitored using a communicating pipe.

For the sealing of a damaged lung, a hole with a diameter of 15 mm was made in a porcine lung. Air was pumped into the lung through an air source (SPB-2, BCHP, China), and the volume of the lung barely increased due to air leakage. Then, Electro-Ox hydrogel tape (diameter: 30 mm) was applied to the hole and waited for 30 s. When air was pumped into the lung again, air leakage stopped. The volume of the lung was monitored using image analysis with ImageJ software.

For the adhesion of a flexible strain sensor, hydrogel tape was applied to the surface of a heart, and a strain sensor was adhered to the hydrogel tape patch. Then, the sensor was connected to an LCR meter (HIOKI-IM3536, Japan), and the heart was made to beat under intermittent airflow. The deformation of the heart was monitored via the capacitance change in the strain sensor.

In vivo adhesion tests

For in vivo adhesion on the gastrocnemius, hydrogels with a width of 5 mm and length of 10 mm were prepared prior to implantation. Then, rabbits (New Zealand rabbit, n=3) were anaesthetized with isoflurane. The hair was removed before the operation. The skin of the gastrocnemius was cut, and hydrogel tape adhesion was achieved through a 2.5 cm incision. Then, the wound was stitched using interrupted sutures (3-0 Vicryl Plus, JNJ). After 3 days, the wound was opened in the same region, and images were taken.

For in vivo adhesion on a beating heart, hydrogel tapes with a diameter of 9 mm were prepared prior to implantation. Then, rabbits were anaesthetized with isoflurane. The chest hair was removed before the operation, and the regional nerve blocker lidocaine/bupivacaine was injected at the surgical site. A thoracotomy was conducted in the third or fourth left intercostal space to expose the heart. The Electro-Ox hydrogel tape was first adhered to the surface of the heart. Then, a metal disk with a diameter of 9 mm and thickness of 1 mm was adhered to the hydrogel tape. The rabbit was ventilated with 100% oxygen for 3 hours and then sacrificed by CO_2 inhalation.

For haemostasis of a bleeding vessel, a pig was anaesthetized with isoflurane. Then, the hair on the neck was removed, and an incision was made to expose the jugular vessel. The vessel was cut, and blood immediately spouted out. Hydrogel tape was pressed to the vessel for 15 s, and the bleeding immediately stopped.

All animal studies were carried out in compliance with the regulations and guidelines of the Ethics Committee of Drum Tower Hospital affiliated to the Medical School of Nanjing University and conducted according to the Institutional Animal Care and Use Committee (IACUC) guidelines.

Statistical significance was determined using Student's t-test, or one-way ANOVA accordingly. Statistical significance was set to a P value <0.05.

Declarations

Data availability

All data are available in the main text or the Supplementary Information

Acknowledgments This work is supported mainly by the National Key R&D Program of China (Grant No.2020YFA0908100), the National Natural Science Foundation of China (No. 11804148, 11674153 and 12002149), the Natural Science Foundation of Jiangsu Province (No. BK20180320), the Fundamental Research Funds for the Central Universities (No. 020414380187, 020414380148 and 020414380138) and the Technological Innovation Foundation of Nanjing University (020414913413).

Author contributions Y. C. and W. W. conceived the idea and designed the study. B. X. and J. G. performed the experiments and analyzed the results. W. Y. prepared some of the hydrogel samples. J. G., L. L. and Q. J. performed the in vitro experiments. Y. C., W. W. and B. X. wrote and refined the paper. Y. C., W. W. and M. Q. supervised the project. All the authors discussed the results.

Competing interests: The authors declare that they have no competing interests.

Supplementary Information is available for this paper.

Correspondence and requests for materials should be addressed to Y. Cao.

Reprints and permissions information is available at http://www.nature.com/reprints.

Ethics: The experimental procedures for all animal studies were reviewed and approved by the Ethics Committee of Drum Tower Hospital affiliated to the Medical School of Nanjing University and conducted according to the Institutional Animal Care and Use Committee (IACUC) guidelines.

References

1 Boutry, C. M. *et al.* A stretchable and biodegradable strain and pressure sensor for orthopaedic application. *Nat. Electron.* **1**, 314-321 (2018).

2 Boutry, C. M. *et al.* Biodegradable and flexible arterial-pulse sensor for the wireless monitoring of blood flow. *Nat. Biomed. Eng.* **3**, 47-57 (2019).

3 Fan, H. & Gong, J. P. Fabrication of Bioinspired Hydrogels: Challenges and Opportunities. *Macromolecules* **53**, 2769-2782 (2020).

4 Sun, J. *et al.* Fabrication and Mechanical Properties of Engineered Protein-Based Adhesives and Fibers. *Adv. Mater.* **32**, 1906360 (2020).

5 Fan, H., Wang, J. & Gong, J. P. Barnacle Cement Proteins-Inspired Tough Hydrogels with Robust, Long-Lasting, and Repeatable Underwater Adhesion. *Adv. Funct. Mater.* **31**, 2009334 (2021).

6 Cui, C. & Liu, W. Recent advances in wet adhesives: Adhesion mechanism, design principle and applications. *Prog. Polym. Sci.* **116**, 101388 (2021).

7 Chang, E. I. *et al.* Vascular anastomosis using controlled phase transitions in poloxamer gels. *Nat. Med.* **17**, 1147-1152 (2011).

8 Shagan, A. *et al.* Hot Glue Gun Releasing Biocompatible Tissue Adhesive. *Adv. Funct. Mater.* **30**, 1900998 (2019).

9 Mehdizadeh, M. & Yang, J. Design Strategies and Applications of Tissue Bioadhesives. *Macromol. Biosci.* **13**, 271-288 (2013).

10 Ramesh, M. & Kumar, L. R. in Green Adhesives. 145-164 (2020)

11 Schricker, S. R. in *Encyclopedia of Nanotechnology.* 1-10 (2014).

12 Zhu, W., Chuah, Y. J. & Wang, D.-A. Bioadhesives for internal medical applications: A review. *Acta Biomater.* **74**, 1-16 (2018).

13 Moulay & Saad. Dopa/Catechol-Tethered Polymers: Bioadhesives and Biomimetic Adhesive Materials. *Polym. Rev.* **54**, 436-513 (2014).

14 Forooshani, P. K. & Lee, B. P. Recent approaches in designing bioadhesive materials inspired by mussel adhesive protein. *J. Polym. Sci. Pol. Chem.* **55**, 9-33 (2017).

15 Balkenende, D. W. R., Winkler, S. M. & Messersmith, P. B. Marine-inspired polymers in medical adhesion. *Eur. Polym. J.* **116**, 134-143 (2019).

16 Matos-Perez, C. R., White, J. D. & Wilker, J. J. Polymer Composition and Substrate Influences on the Adhesive Bonding of a Biomimetic, Cross-Linking Polymer. *J. Am. Chem. Soc.* **134**, 9498-9505 (2012).

17 Bu, Y. *et al.* Tetra-PEG Based Hydrogel Sealants for In Vivo Visceral Hemostasis. *Adv. Mater.* **31**, 1901580 (2019).

18 Wang, Z., Guo, L., Xiao, H., Cong, H. & Wang, S. A reversible underwater glue based on photo- and thermo-responsive dynamic covalent bonds. *Mater. Horiz.* **7**, 282-288 (2020).

19 Leggat, P. A., Smith, D. R. & Kedjarune, U. SURGICAL APPLICATIONS OF CYANOACRYLATE ADHESIVES: A REVIEW OF TOXICITY. *ANZ J. Surg.* **77**, 209-213 (2007).

20 MacGillivray, T. E. Fibrin Sealants and Glues. *J. Cardiac Surg.* **18**, 480-485 (2003).

21 Zhang, Y. S. & Khademhosseini, A. Advances in engineering hydrogels. *Science* **356**, eaaf3627 (2017).

22 Ghobril, C. & Grinstaff, M. W. The chemistry and engineering of polymeric hydrogel adhesives for wound closure: a tutorial. *Chem. Soc. Rev.* **44**, 1820-1835 (2015).

23 Shin, J. *et al.* Tissue Tapes—Phenolic Hyaluronic Acid Hydrogel Patches for Off-the-Shelf Therapy. *Adv. Funct. Mater.* **29**, 1903863 (2019).

24 Zhao, Y. *et al.* Bio-inspired reversible underwater adhesive. *Nat. Commun.* **8**, 2218 (2017).

25 Bradley, L. C. *et al.* Rough Adhesive Hydrogels (RAd gels) for Underwater Adhesion. *ACS Appl. Mater. Inter.* **9**, 27409-27413 (2017).

26 Fan, H. *et al.* Adjacent cationic–aromatic sequences yield strong electrostatic adhesion of hydrogels in seawater. *Nat. Commun.* **10**, 5127 (2019).

27 Han, L., Wang, M., Prieto-López, L. O., Deng, X. & Cui, J. Self-Hydrophobization in a Dynamic Hydrogel for Creating Nonspecific Repeatable Underwater Adhesion. *Adv. Funct. Mater.* **30**, 1907064 (2020).

28 Balkenende, D. W. R., Winkler, S. M., Li, Y. & Messersmith, P. B. Supramolecular Cross-Links in Mussel-Inspired Tissue Adhesives. *ACS Macro Lett.* **9**, 1439-1445 (2020).

29 Yuk, H. *et al.* Dry double-sided tape for adhesion of wet tissues and devices. *Nature* **575**, 169-174 (2019).

30 Liu, J. *et al.* Fatigue-resistant adhesion of hydrogels. *Nat. Commun.* **11**, 1071 (2020).

31 Liu, X., Zhang, Q., Qiao, Y., Duan, L. & Gao, G. Anti-fatigue adhesive and tough hydrogels regulated by adenine and uracil. *Polym. Chem.* **9**, 4535-4542 (2018).

32 Pinnaratip, R., Bhuiyan, M. S. A., Meyers, K., Rajachar, R. M. & Lee, B. P. Multifunctional Biomedical Adhesives. *Adv. Health. Mater.* **8**, 1801568 (2019).

33 Bouten, P. J. M. *et al.* The chemistry of tissue adhesive materials. *Prog. Polym. Sci.* **39**, 1375-1405 (2014).

34 Duarte, A. P., Coelho, J. F., Bordado, J. C., Cidade, M. T. & Gil, M. H. Surgical adhesives: Systematic review of the main types and development forecast. *Prog. Polym. Sci.* **37**, 1031-1050 (2012).

35 Deng, J. *et al.* Electrical bioadhesive interface for bioelectronics. *Nat. Mater.* **20**, 229–236 (2020).

36 Gao, Y., Wu, K. & Suo, Z. Photodetachable Adhesion. *Adv. Mater.* **31**, 1806948 (2019).

37 Chen, X., Yuk, H., Wu, J., Nabzdyk, C. S. & Zhao, X. Instant tough bioadhesive with triggerable benign detachment. *P. Natl. Acad. Sci. USA* **117**, 15497-15503 (2020).

38 Li, Y. R. *et al.* Molecular design principles of Lysine-DOPA wet adhesion. *Nat. Commun.* **11** (2020).

39 Li, Y. & Cao, Y. The molecular mechanisms underlying mussel adhesion. *Nanoscale Adv.* **1**, 4246-4257 (2019).

40 Delparastan, P., Malollari, K. G., Lee, H. & Messersmith, P. B. Direct Evidence for the Polymeric Nature of Polydopamine. *Angew. Chem. Int. Edit.* **58**, 1077-1082 (2019).

41 Russell *et al.* Natural underwater adhesives. *J. Polym. Sci., Part B: Polym. Phys.* **49**, 757-771 (2011).

42 Ahn, B. K., Lee, D. W., Israelachvili, J. N. & Waite, J. H. Surface-initiated self-healing of polymers in aqueous media. *Nat. Mater.* **13**, 867-872 (2014).

43 Li, Y. R. *et al.* Single-molecule study of the synergistic effects of positive charges and Dopa for wet adhesion. *J. Mater. Chem. B* **5**, 4416-4420 (2017).

44 Li, Y. R. *et al.* Single-Molecule Force Spectroscopy Reveals Multiple Binding Modes between DOPA and Different Rutile Surfaces. *Chemphyschem* **18**, 1466-1469 (2017).

45 Li, Y. R. *et al.* Single-Molecule Mechanics of Catechol-Iron Coordination Bonds. *ACS. Biomater. Sci. Eng.* **3**, 979-989 (2017).

46 Li, Y. R., Qin, M., Li, Y., Cao, Y. & Wang, W. Single Molecule Evidence for the Adaptive Binding of DOPA to Different Wet Surfaces. *Langmuir* **30**, 4358-4366 (2014).

47 Trexler, M. M. *et al.* Synthesis and mechanical properties of para-aramid nanofibers. *J. Polym. Sci., Part B: Polym. Phys.* **57**, 563-573 (2019).

48 Lee, B. P., Dalsin, J. L. & Messersmith, P. B. Synthesis and Gelation of DOPA-Modified Poly(ethylene glycol) Hydrogels. *Biomacromolecules* **3**, 1038-1047 (2002).

49 Petran, A., Popa, A., Hădade, N. D. & Liebscher, J. New Insights into Catechol Oxidation – Application of Ammonium Peroxydisulfate in the Presence of Arylhydrazines. *ChemistrySelect* **5**, 9523-9530 (2020).

50 Yang, Z. *et al.* Highly Stretchable, Adhesive, Biocompatible, and Antibacterial Hydrogel Dressings for Wound Healing. *Adv. Sci.* **8**, 2003627 (2020).

51 Gan, D. *et al.* Plant-inspired adhesive and tough hydrogel based on Ag-Lignin nanoparticles-triggered dynamic redox catechol chemistry. *Nat. Commun.* **10**, 1487 (2019).

52 Wei, K. *et al.* Mussel-Inspired Injectable Hydrogel Adhesive Formed under Mild Conditions Features Near-Native Tissue Properties. *ACS Appl. Mater. Inter.* **11**, 47707-47719 (2019).

53 Annabi, N. *et al.* Engineering a sprayable and elastic hydrogel adhesive with antimicrobial properties for wound healing. *Biomaterials* **139**, 229-243 (2017).

54 Yang, B. *et al.* Injectable Adhesive Self-Healing Multicross-Linked Double-Network Hydrogel Facilitates Full-Thickness Skin Wound Healing. *ACS Appl. Mater. Inter.* **12**, 57782-57797 (2020).

55 Cui, C. *et al.* A Janus Hydrogel Wet Adhesive for Internal Tissue Repair and Anti-Postoperative Adhesion. *Adv. Funct. Mater.* **30**, 2005689 (2020).

56 Qiang *et al.* A Robust, One-Pot Synthesis of Highly Mechanical and Recoverable Double Network Hydrogels Using Thermoreversible Sol-Gel Polysaccharide. *Adv. Mater.* **25**, 4171-4176 (2013).

57 Highly Elastic and Ultratough Hybrid Ionic–Covalent Hydrogels with Tunable Structures and Mechanics. *Adv. Mater.* **30**, 1707071 (2018).

58 Yuk, H., Zhang, T., Lin, S., Parada, G. A. & Zhao, X. Tough bonding of hydrogels to diverse non-porous surfaces. *Nat. Mater.* **15**, 190-196 (2016).

59 Li, J. *et al.* Tough adhesives for diverse wet surfaces. *Science* **357**, 378-381 (2017).

Figures

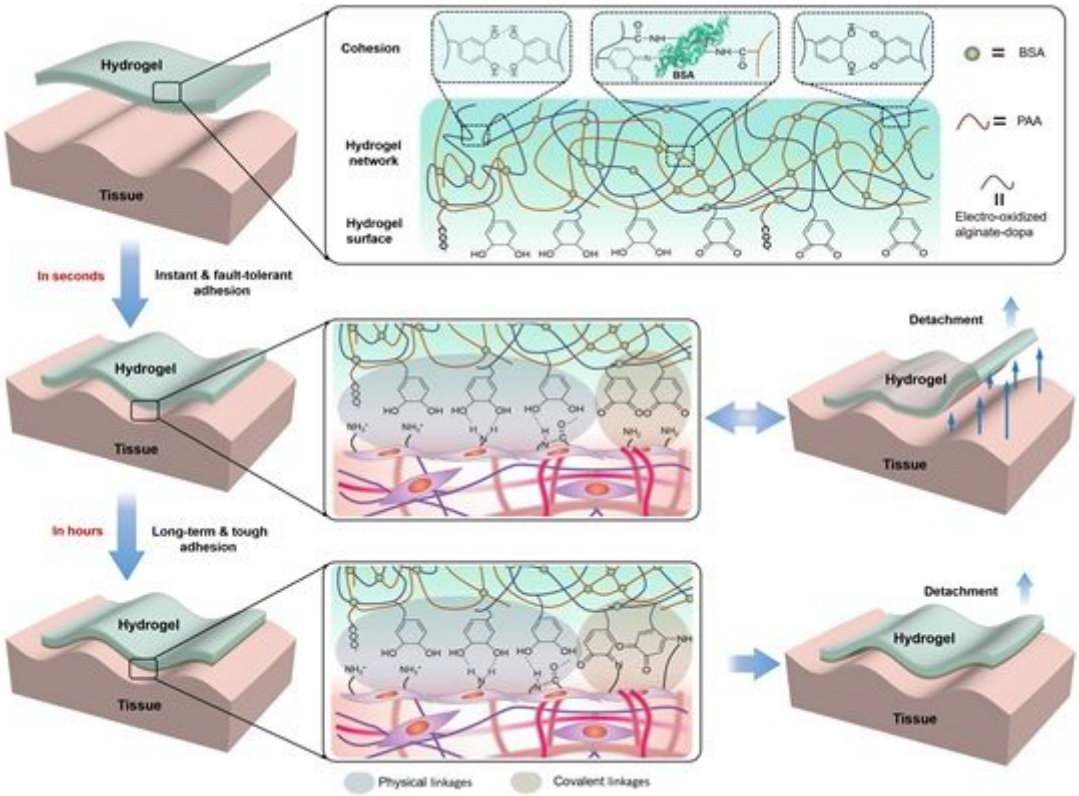

Figure 1

Schematic illustration of the crosslinking and adhesion mechanism of Electro-Ox hydrogel tape. The hydrogel is mainly crosslinked by covalent bonds between BSA and electro-oxidized alginate-dopa or PAA formed via EDC-NHS. The conjugation between amine groups from BSA and dopaquinone generated during electro-oxidation further strengthens the hydrogel tapes. The unfolding of BSA and rupture of hydrogen bonds between dopa/dopaquinone can dissipate considerable energy and endow the hydrogel tape with high toughness. The adhesion between the hydrogel tape and tissue surface is time dependent. First, mainly non-covalent interactions (ionic interactions, cation-π interactions and hydrogen bonds) are formed in seconds. As the reaction between amines from the tissue surface and dopaquinone in the hydrogel proceeds, the surface bonding is gradually enhanced in hours.

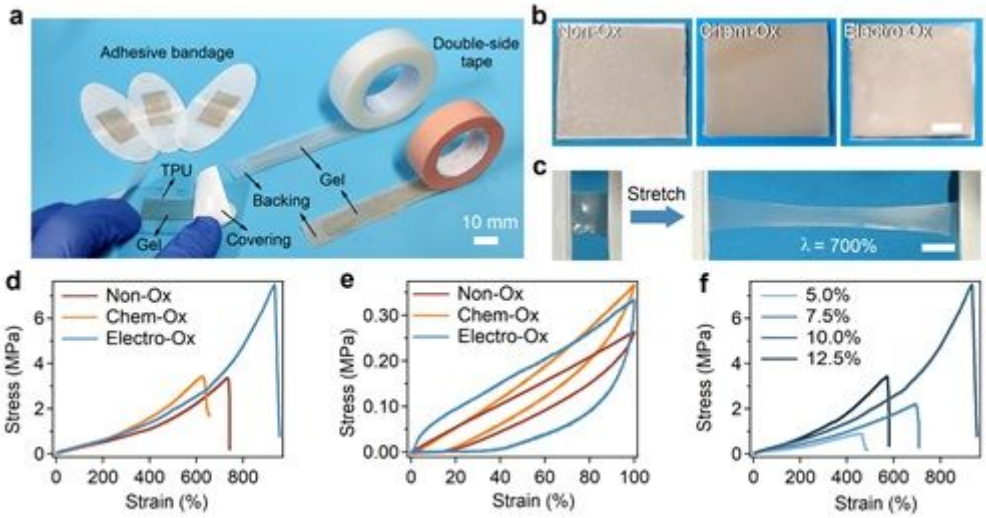

Figure 2

Mechanical properties of the adhesive hydrogel tapes based on electro-oxidized alginate-dopa. a, Adhesive bandages and double-side tapes made of Electro-Ox hydrogels. b, Images of the Non-Ox, Chem-Ox and Electro-Ox hydrogel tapes on white patches. Scale bar = 10 mm. c, Images of the Electro-Ox hydrogel tape stretched to more than 7 times the original length. Scale bar = 10 mm. d, Typical tensile stress-strain curves of the Non-Ox, Electro-Ox and Chem-Ox hydrogel tapes at an alginate-dopa concentration of 10 w/v%. e, Typical stretch-relaxation curves of Non-Ox, Chem-Ox and Electro-Ox hydrogel tapes. f, Typical tensile stress-strain curves of Electro-Ox hydrogel tapes at various mass concentrations of electro-oxidized alginate-dopa (5.0, 7.5, 10.0 and 12.5 w/v%).

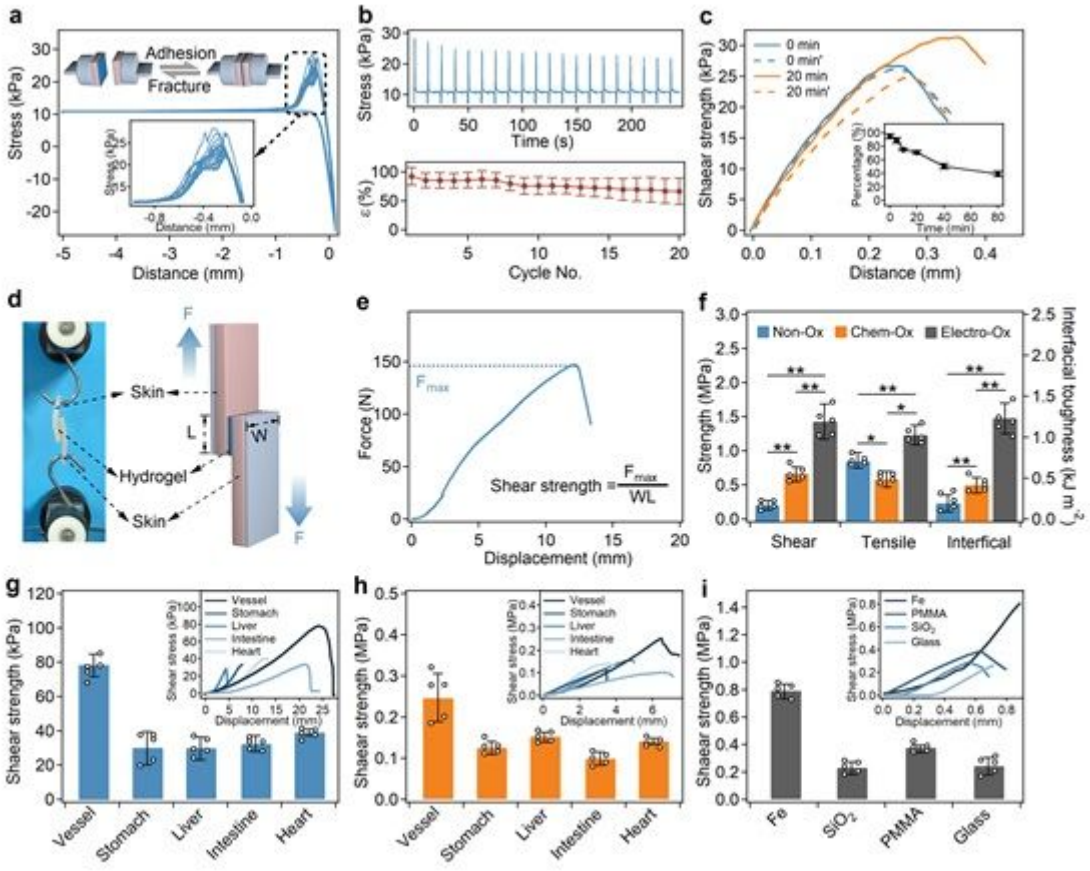

Figure 3

Adhesion performance of the Electro-Ox hydrogel tape. a, Cyclic compression and fracture curves versus displacement of instant adhesion for porcine skin using Electro-Ox hydrogel tape in 20 cycles. The top inset corresponds to a schematic of the compression and fracture cycles. The bottom inset corresponds to the magnified fracture curves. b, Cyclic compression and fracture curves versus time (top) and normalized tensile strength (ε, bottom) of instant adhesion for porcine skin using Electro-Ox hydrogel tape in 20 cycles. c, Typical lap shear curves of instant adhesion (0 min), adhesion after the fracture of initial adhesion (0 min'), adhesion after curing for 20 min (20 min) and instant adhesion after the fracture of 20 min adhesion (20 min'). The inset corresponds to the normalized tensile strength of a second instant adhesion event after different times (normalized 0 min', 5 min', 10 min', 20 min', 40 min' and 80 min'). d, Image and schematic for the measurement of shear strength based on the standard lap shear test. F, force; W, width; L, length. e, Typical force-displacement curve recorded in the lap shear test and the determination of shear strength. f, Shear strength, tensile strength and interfacial toughness of long-term adhesion for different hydrogels. g, h, Shear strength of short-term (g) and long-term (h) adhesion for different porcine organs using Electro-Ox hydrogel tape. i, Shear strength of long-term adhesion for different substrates (Fe, SiO2, PMMA and glass) using Electro-Ox hydrogel tape. Values represent the mean and standard deviation (n=5). **: $p < 0.01$, *: $p < 0.05$.

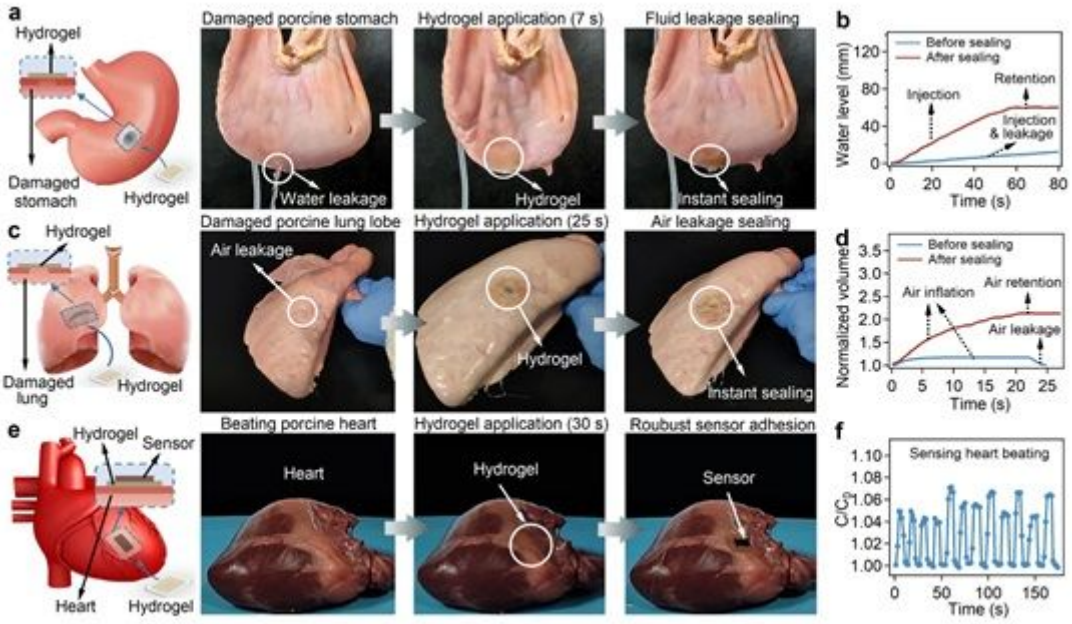

Figure 4

Applications of the Electro-Ox hydrogel tape to tissue adhesion. a, Sealing of a water-leaking fresh porcine stomach using Electro-Ox hydrogel tape. b, Water level in the stomach corresponding to the sealing process in a. c, Sealing of an air-leaking fresh porcine lung using Electro-Ox dopa hydrogel tape. d, Volume change in the lung corresponding to the sealing process in c. e, Electro-Ox hydrogel tape-mediated adhesion of a hydrogel-based strain sensor on a beating porcine heart driven by an air pump. f, Normalized capacitance (C/C0) of the strain sensor adhered to the porcine heart over time corresponding to mimicked heart beating in e.

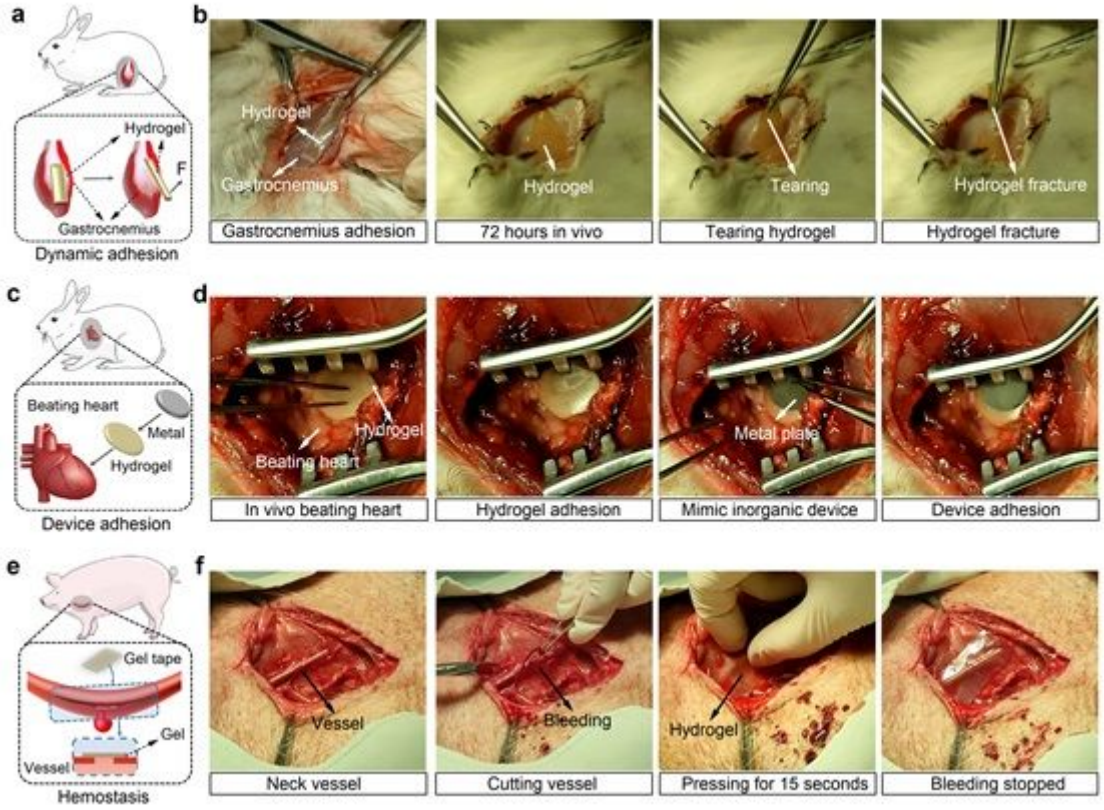

Figure 5

In vivo adhesion and haemostasis of Electro-Ox hydrogel tape. a, Schematic illustration of adhesion on rabbit gastrocnemius. b, Adhesion of Electro-Ox hydrogel tape on rabbit gastrocnemius before and after 72 hours in vivo. c, Schematic illustration of device adhesion on a beating rabbit heart. d, Adhesion of a metal sheet on a beating rabbit heart via Electro-Ox hydrogel tape in vivo. e, Schematic illustration of haemostasis on the bleeding carotid artery of a pig. f, Haemostasis of the bleeding carotid artery of a pig using Electro-Ox hydrogel tape in vivo.

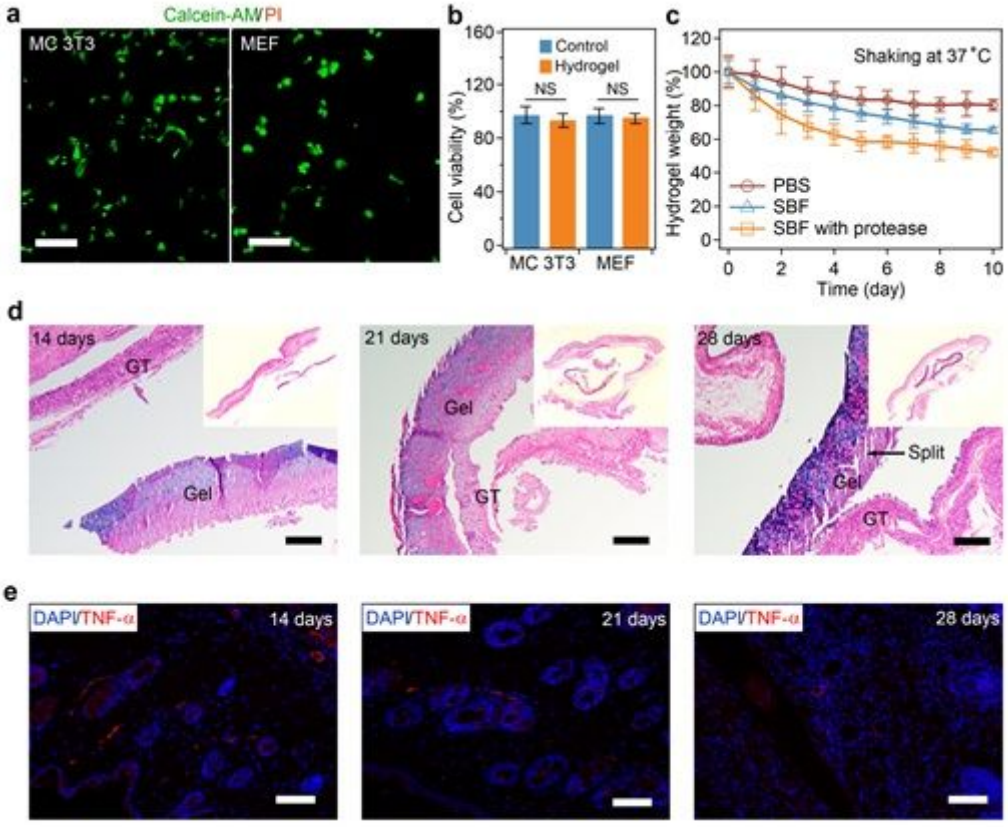

Figure 6

Biocompatibility and biodegradability of Electro-Ox hydrogel tape in vitro and in vivo. a, b, Fluorescence microscopy images (a) and cell viability (b) of MC 3T3 and MEF cells cultured on Electro-Ox hydrogel. The living and dead cells were stained with a live/dead assay (Calcein-AM/PI Double Staining Kit) after 24 h of culture. NS: $p > 0.05$. c, In vitro biodegradation of Electro-Ox hydrogel tape in SBF with or without protease. Values in a-c represent the mean and standard deviation (n = 5-7). d, Representative histological images stained with haematoxylin and eosin (H&E) for assessment of the biodegradation of the Electro-Ox hydrogel tape in vivo after subcutaneous implantation for 14, 21 and 28 days. All experiments were repeated at least three times with similar results. Scale bar = 400 μm. e, Representative images identified by molecular marker (TNF-α) immunostaining for assessment of the inflammatory responses to the Electro-Ox hydrogel tape in vivo after subcutaneous implantation for 14, 21 and 28 days. TNF-α (red), a specific marker of inflammation, was not obvious in any of the images. Cell nuclei are indicated by 4',6-diamidino-2-phenylindole (DAPI, blue). Scale bar = 100 μm. All experiments were repeated at least three times with similar results.

Supplementary Files

This is a list of supplementary files associated with this preprint. Click to download.

- MovieS1.mp4
- MovieS2.mp4

- MovieS3.mp4
- MovieS4.mp4
- MovieS5.mp4
- MovieS6.mp4
- SIHydrogeltapesforfaulttolerantstrongwetadhesion.docx